




Carnot, Stirling, and Ericsson stochastic heat engines: Efficiency at maximum powerO. Contreras-Vergara and N. Sánchez-Salas *Departamento de Física, Escuela Superior de Física y Matemáticas, Instituto Politécnico Nacional, Edif. 9 UP Zacatenco, CP 07738, CDMX, México*G. Valencia-Ortega *División de Matemáticas e Ingeniería, Facultad de Estudios Superiores Acatlán, Universidad Nacional Autónoma de México, Av. Alcanfores y San Juan Totoltepec, Santa Cruz Acatlán, Naucalpan de Juárez, 53150, Estado de México, México*J. I. Jiménez-Aquino *Departamento de Física, Universidad Autónoma Metropolitana–Iztapalapa, C.P. 09340, CDMX, México*

(Received 9 November 2022; revised 5 April 2023; accepted 26 June 2023; published 21 July 2023)

This work uses the low-dissipation strategy to obtain efficiency at maximum power from a stochastic heat engine performing Carnot-, Stirling- and Ericsson-like cycles at finite time. The heat engine consists of a colloidal particle trapped by optical tweezers, in contact with two thermal baths at different temperatures, namely hot (T_h) and cold (T_c). The particle dynamics is characterized by a Langevin equation with time-dependent control parameters bounded to a harmonic potential trap. In a low-dissipation approach, the equilibrium properties of the system are required, which in our case, can be calculated through a state-like equation for the mean value $\langle x^2 \rangle_{\text{eq}}$ coming from a macroscopic expression associated with the Langevin equation.

DOI: [10.1103/PhysRevE.108.014123](https://doi.org/10.1103/PhysRevE.108.014123)**I. INTRODUCTION**

With the use of nanotechnology, physicists and engineers attempt to overcome the challenge of building artificial mesoscopic machines capable of extracting energy from their environment, and converting it into useful work. The main characteristic of these micro or nanoengines is that the fluctuations generated by their environment is comparable to the average flow of energy produced by such engines. Then, the performance of a mesoscopic engine strongly depends on the properties of its surroundings. For instance, the so-called Brownian motors [1–3] are devices capable of rectifying fluctuations to produce useful work; they have a ratchetlike design in which a spatial anisotropic or asymmetric potential is involved, and an additional ingredient that takes the system out of equilibrium. As has been shown, an equivalent performance for these devices can be obtained if the system is coupled to two thermal baths simultaneously or if an external parameter is modulated [4,5].

The ratchet model proposed by Feynman has been used as an inspiration for the study of a significant number of theoretical and experimental works on Brownian motors and other devices [1–3,6–16], such as the stochastic heat engines in the construction of microscopic devices. The first experimental realization of a microscopic heat engine consisting of a Brownian particle in a time-dependent optical trap was reported in [17]. In this experiment, the Brownian particle performs a Stirling-like cycle, in which the particle and the trapping potential replace the working fluid, and the piston of its macroscopic counterpart. The technique of trapping particles using optical tweezers has been shown to provide a

precise control over the confinement and temperature of the colloidal particle [18,19], wherein isothermal and nonisothermal processes are following in this cycle [19–22].

The two fundamental quantities used to characterize the thermodynamic properties of macroscopic and microscopic heat engines are both power and efficiency. The main difference between both engines is that in the latter the stochastic fluctuations play a fundamental role. Nowadays, stochastic thermodynamics has been the appropriate theoretical framework to characterize the energetics of microscopic heat engines in which the concepts of work, heat, internal energy, etc., have been defined along a single stochastic trajectory [23].

It is well known that for macroscopic heat engines, the Carnot efficiency can be achieved when the cyclic process is quasistatic, which also means a large cycle time and zero power output. The so-called finite-time thermodynamics is related to the study of the efficiency of heat engines when the cyclic process is performed at finite-time. It seems that the pioneering work related to the efficiency at maximum power of an endoreversible engine operating at finite time was reported by Novikov [24]. However, the paper by Curzon and Ahlborn [25] is more cited in literature, in which the efficiency at maximum power is shown to satisfy $\eta_{\text{CA}} = 1 - \sqrt{T_c/T_h}$, which is less than the Carnot efficiency $\eta_{\text{CA}} < \eta_c$, for an engine operating between two heat baths at temperatures T_h and T_c ($T_c < T_h$). Since then, a significant number of papers related to Finite-Time Thermodynamics have been reported in literature [26–29], and all references therein.

In this context, it is worth highlighting the paper by Esposito *et al.* [30], related to the efficiency at maximum power

for macroscopic heat engines performing finite-time Carnot cycles, and operating under low dissipation conditions. According to the authors, the starting point of low-dissipation approach is a Carnot engine which operates under reversible conditions while the system always remains close to equilibrium, and the cycle time becomes very large. If the cyclic processes are no longer reversible, but irreversible at finite-time, then the dissipative processes play an important role, the low-dissipation limit being an interesting theoretical approach to characterize them. This approach establishes that if τ_c (τ_h) is the time in which the system is in contact with the cold (hot) reservoir along a cycle, then the entropy production along the cold (hot) part of the cycle is proposed to behave as Σ_c/τ_c (Σ_h/τ_h), where Σ contains information about the irreversibilities present at isothermal branches. Therefore, the amounts of heat per cycle incoming to the system from the cold (hot) reservoir are given by $Q_c = T_c(-\Delta S - \Sigma_c/\tau_c + \dots)$ and $Q_h = T_h(\Delta S - \Sigma_h/\tau_h + \dots)$, being $Q_\infty^c = -T_c\Delta S$ and $Q_\infty^h = T_h\Delta S$, the heat exchanged with the cold (hot) reservoir under reversible conditions. Whereas, the adiabatic processes are considered as instantaneous, therefore the irreversible effects are only taken into account in the two isothermal processes.

The study of the efficiency at maximum power has also been extended to stochastic heat engines, as can be corroborated in recent literature [17,31–34]. Due to the aforementioned features of a stochastic heat engine, the theoretical model used for its description is the Langevin equation in which the optical trap is represented by a harmonic potential. The model also considers the engine (the particle) in contact with two thermal baths at different temperatures T_h (hot) and T_c (cold), with $T_h > T_c$, and the internal noise intensity changes in time from the hot to cold values. The stochastic efficiency is also defined as the ratio of the extracted work and the heat transferred from the hot bath to the particle in a cycle [19]. In a work by Blickle [17], it was shown that at thermodynamic level the mean efficiency $\langle\eta(\tau)\rangle$ is less than the Carnot efficiency $\eta_c = 1 - T_c/T_h$, that is $\langle\eta(\tau)\rangle = \langle W(\tau)\rangle/\langle Q(\tau)\rangle < \eta_c$, where τ is the cycle time, $\langle W(\tau)\rangle$ the average work, and $\langle Q(\tau)\rangle$ the average heat flux. Also, the experiments [17,19] show that for shorter cycle times, the dissipation effects become important, and the mean work per cycle can be written as $\langle W\rangle = \langle W\rangle_\infty + \langle W\rangle_{\text{dis}}$, where $\langle W\rangle_\infty$ is the mean quasistatic work for longer cycle times and $\langle W\rangle_{\text{dis}}$ the mean dissipated work per cycle. The latter is proposed to first order as $\langle W\rangle_{\text{dis}} = \Sigma/\tau$, where Σ is a parameter which contains information about the irreversibilities present in the cycle, or in other words, it accounts for an amount of energy dissipated in a cycle. In [17] it has also been commented that, in the experiment at small scales it is very difficult to keep hot and cold reservoirs thermally isolated, so rather than coupling the colloidal particle periodically to different heat baths, the temperature of the surrounding liquid is suddenly changed.

The purpose of the present contribution is to apply the low-dissipation considerations to obtain the efficiency at maximum power of a Brownian heat engine, which can operate in three finite-time irreversible cycles between a hot and a cold reservoir at temperatures T_h and T_c , respectively. Three different cycles, namely Carnot-, Stirling-, and Ericsson-like,

are considered. The theoretical analysis is formulated in the context of a Langevin approach for a Brownian particle in a harmonic trap with time-dependent stiffness $\kappa(t)$. The strategy is as follows: first, the Langevin equation is transformed into a macroscopic one for the average value $\langle x^2(t)\rangle$, in which the time-dependent temperature $T(t)$ is also taken into account (both the stiffness and temperature are externally controlled [35]). Instead of solving the macroscopic deterministic equation for specific protocols, $\kappa(t)$ and $T(t)$, the advantage from the system equilibrium thermodynamic properties is taken into account by means of the *statelike equation* associated with the average value $\langle x^2\rangle_{\text{eq}}$. This allows obtaining the work, heat, and efficiency under quasistatic conditions, and all the irreversible effects are taken into account through the dissipation parameter Σ [17]. Once this is done, the efficiency at maximum power characterized by finite-time cycles can be obtained using the low-dissipation approach.

This work is organized as follows. Section II obtains the macroscopic equation for the average value $\langle x^2(t)\rangle$, coming from the overdamped harmonic oscillator Langevin equation. The law of energy balance according to Sekimoto is presented to get the average of the total energy. In Sec. III the equilibrium thermodynamic properties for the Carnot-, Stirling-, and Ericsson-like cycles are calculated by means of a statelike equation coming from the macroscopic equation associated with $\langle x^2\rangle$. Section IV focuses on the study of low-dissipation approach to calculate the efficiency at maximum power of each heat engine, and the theoretical results are compared with other reported results. The conclusions and comments are given in Sec. V.

II. STOCHASTIC HEAT ENGINE

Usually the mathematical model proposed to describe the dynamics of a Brownian heat engine in contact with a heat bath of temperature T is given by a Langevin equation associated with a Brownian particle in a harmonic potential trap with stiffness κ , $U(x) = \frac{1}{2}\kappa x^2$. The Langevin equation can be written as

$$m\frac{d^2x}{dt^2} = -\gamma\frac{dx}{dt} - \kappa x + \xi(t), \quad (1)$$

where the noise term $\xi(t)$ is Gaussian with zero mean value and correlation function $\langle \xi(t)\xi(t')\rangle = \gamma k_b T \delta(t - t')$, with k_b the Boltzmann constant, m the particle mass, $\gamma = 6\pi\zeta a$ the friction coefficient, ζ the fluid viscosity, and a the radius of the particle assumed to be a sphere. In the overdamped regime it becomes

$$\gamma\frac{dx}{dt} = -\kappa x + \xi(t). \quad (2)$$

This equation can easily be transformed into a macroscopic one for the average value $\langle x^2\rangle$, that is

$$\gamma\frac{d\langle x^2\rangle}{dt} = -2\kappa\langle x^2\rangle + 2\langle x\xi(t)\rangle. \quad (3)$$

With the solution of Eq. (2) together with the noise correlation function it can be shown that $\langle x\xi(t)\rangle = k_b T$, and thus, the

macroscopic equation now reads

$$\gamma \frac{d\langle x^2 \rangle}{dt} = -2\kappa \langle x^2 \rangle + 2k_B T. \quad (4)$$

It is also clear that in the long time limit, this process reaches its equilibrium stationary state, and therefore $\langle x^2 \rangle_{\text{eq}} = k_B T / \kappa$.

On the other hand, according to Sekimoto [23], the law of energy balance along a single stochastic trajectory is related to the amount of work and heat exchanged by a Brownian particle with its surroundings (heat bath). In the overdamped regime, Sekimoto shows (in Sec. 4.1.3.2 of his book [23]) that the average of heat $d'Q$ over stochastic processes between t and $t + dt$ for a particular harmonic potential is given by

$$\langle d'Q \rangle = \left[-\frac{\kappa^2}{\gamma} \langle x^2 \rangle + \frac{\kappa^2}{\gamma} k_B T \right] dt. \quad (5)$$

Substituting the solution of Eq. (4), it is easy to show that the average of the total heat exchanged with the surroundings becomes $\langle Q \rangle = \frac{1}{2} k_B T$. Hence, even in the overdamped regime, the total energy is $E = U + \frac{1}{2} k_B T$.

Returning to Brownian heat engines, it is worth mentioning that the construction of Brownian heat engines is already possible, as can be corroborated in Refs. [17,19,20]. The main characteristic of such heat engines is the external time-dependent control of both the stiffness of the harmonic potential trap and heat bath temperature. This fact allows that the single Brownian particle can perform a nonequilibrium cyclic process during a finite time, which is the case of the stochastic Stirling-like [17] and Carnot-like cycles [20].

In recent papers [13,33,34,36,37], the amount of work, the exchange of heat with the thermal bath, as well as the efficiency at maximum power performed by a Brownian heat engine during a cycle are calculated along a single stochastic trajectory, taking into account a specific form of the time-dependent protocol $\kappa(t)$ and temperature $T(t)$ using the Langevin and Fokker-Planck theoretical approach. Our present contribution calculates the efficiency at maximum power of three stochastic heat engines using an alternative strategy related only to the Langevin dynamics, and low-dissipation approach. For this purpose the following is considered when both the stiffness of the optical trap, as well as the temperature are time-dependent parameters; the overdamped Langevin equation is written as

$$\gamma \frac{dx}{dt} = -\kappa(t)x + \xi(t), \quad (6)$$

and the noise correlation function is assumed to satisfy $\langle \xi(t)\xi(t') \rangle = \gamma k_B T(t) \delta(t - t')$. Next, the associated macroscopic equation is constructed which becomes

$$\gamma \frac{d\langle x^2 \rangle}{dt} = -2\kappa(t) \langle x^2 \rangle + 2\langle x\xi(t) \rangle. \quad (7)$$

Also, with the solution of Eq. (6) along with the previous noise correlation function, Eq. (7) is now given by

$$\gamma \frac{d\langle x^2 \rangle}{dt} = -2\kappa(t) \langle x^2 \rangle + 2k_B T(t). \quad (8)$$

In principle, given some specific protocol for $\kappa(t)$ and $T(t)$, the nonequilibrium thermodynamic quantities, as the average work $\langle W(\tau) \rangle$, average heat $\langle Q(\tau) \rangle$, etc., during a finite time

τ , can be calculated through the solution of Eq. (8). However, instead of doing this, the advantage from low-dissipation strategy [30] is considered to calculate such nonequilibrium quantities around the equilibrium state. As far as is known, the low-dissipation method reported in [30] has not yet been considered in the study of stochastic heat engines. The proposal allows us to first calculate all the equilibrium thermodynamic properties of the system through the statelike equation coming from Eq. (8).

III. QUASISTATIC DESCRIPTION OF BROWNIAN HEAT ENGINES

The thermodynamic properties of the Brownian heat engine, can be calculated by means of the statelike equation in a similar way as in the case of an ideal gas in classical thermodynamics. It can be seen that in the equilibrium state the stiffness, as well as the temperature proposed in Eq. (8), become constants and the equation of statelike is given by $\langle x^2 \rangle_{\text{eq}} = k_B T / \kappa$. Therefore, a statepoint is characterized by $(\langle x^2 \rangle, \kappa, T)$ as thermodynamic variables. In what follows considers $\langle x^2 \rangle_{\text{eq}} \equiv \langle x^2 \rangle$, the average of the total energy $\langle E \rangle \equiv E$, the average of work $\langle W \rangle \equiv W$, and heat $\langle Q \rangle \equiv Q$ are the same as the thermodynamic quantities. On the other hand, it has been shown above that the total energy E can also be written as

$$E = \frac{1}{2} \kappa \langle x^2 \rangle + \frac{1}{2} k_B T, \quad (9)$$

and thus, $E = k_B T$. Once the energy available by the system is defined, different thermodynamiclike processes can be explored, whereas the Brownian particle is in contact with two thermal baths at different temperatures, hot T_h and cold T_c [17,20,38,39]. To calculate the efficiency at quasistatic conditions for the three aforementioned stochastic heat engines, the following proceeds: the first lawlike of thermodynamics along a stochastic trajectory reads in the overdamped regime as $dE = d'Q + d'W$, where $d'W = \frac{\partial U}{\partial a} \circ da$ (Stratonovich type calculus). In our case $a = \kappa$, and thus $U(x, \kappa) = \frac{1}{2} \kappa x^2$ and $d'W = \frac{1}{2} x^2 d\kappa$. However, according to Eq. (9) it can be shown that $d'Q = \frac{1}{2} \kappa d\langle x^2 \rangle + \frac{1}{2} k_B dT$.

The total work W and exchange heat Q with the surroundings along a quasistatic trajectory, from a one state A to another state B , are respectively given by

$$W_{AB} = \frac{1}{2} \int_A^B \langle x^2 \rangle d\kappa, \quad (10)$$

$$Q_{AB} = \frac{1}{2} \int_A^B \kappa d\langle x^2 \rangle + \frac{1}{2} k_B (T_B - T_A). \quad (11)$$

Moreover, the Brownian particle free energy can be obtained from the partition function given by $Z(\kappa, T) = \sqrt{2\pi k_B T / \kappa}$, hence $F(\kappa, T) = -k_B T \ln \sqrt{2\pi k_B T / \kappa}$. In analogy to the differential form of the thermodynamic potential for an ideal gas $dF = -SdT - pdV$, there is a correspondence with ensembles of a single-confined colloidal particle in the form $dF = -SdT + \Phi d\kappa$, where the entropy S reads $S = -(\frac{\partial F}{\partial T})_\kappa = (k_B/2)[\ln(2\pi k_B T / \kappa) + 1]$, and the auxiliary conjugate thermodynamic variable Φ also satisfies the statelike equation $\Phi = (\frac{\partial F}{\partial \kappa})_T = \frac{k_B T}{2\kappa} = \frac{\langle x^2 \rangle}{2}$. In this equation the trap stiffness

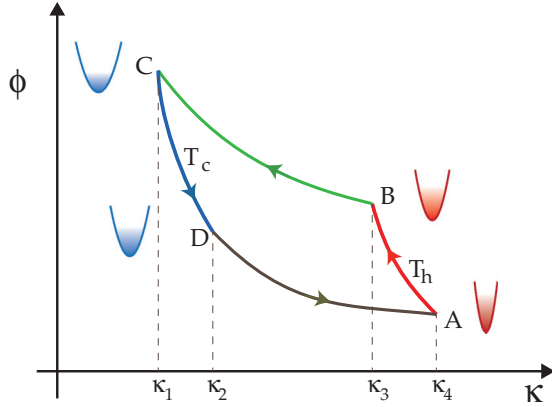


FIG. 1. Φ - κ thermodynamic diagram of a Carnot-like cycle with (i) an isothermal expansion ($A \rightarrow B$ path), (ii) an adiabatic expansion ($B \rightarrow C$ path), (iii) an isothermal compression ($C \rightarrow D$ path), and (iv) an adiabatic compression ($D \rightarrow A$ path).

plays the role of an effective volume in the state equation of an ideal gas $p \sim T/V$, while the intensive variable Φ can be seen as a kind of effective macroscopic pressure. The theoretical study is complemented with the calculation of the adiabaticlike equation associated with the system, which is easily obtained from the condition $d'Q = 0$, yielding to $\kappa = \text{const } T^2$ consistent with the one previously reported in [19,40].

In analogy with real-macroscopic heat engines, the energy conversion efficiency of thermodynamic protocols with single particles in suspension is constrained by the second law of thermodynamics [31,40,41], that is

$$\eta \equiv \frac{\langle W(\tau) \rangle}{\langle Q_h(\tau) \rangle} \leq \eta_c, \quad (12)$$

where η_c is the Carnot efficiency. In thermal equilibrium conditions, i.e., in the quasistatic limit ($\tau \rightarrow \infty$), the efficiency for these types of block-thermodynamic cycle models are close to η_c ; under this condition the power output is zero.

In optically trapped particle systems immersed in a fluid, isothermal processes are associated with the so-called breathing optical parabola [42,43]. That is, as the stiffness of the trap is decreased (increased) space for the particle increases (decreases). Thus, the free energy change, ΔF , stands for the useful reversible work during the expansion and compression processes at fixed temperatures.

A. Carnot-like cycle

The Carnot cycle represents the paradigm of thermal cycles; it consists of two adiabatic and two isothermal branches, whose maximum efficiency is $\eta_c = 1 - T_c/T_h$ under reversible conditions. The Carnot-like cycle for a Brownian particle can be implemented, modifying the stiffness κ and the bath temperature T [19], see Fig. 1. The idealized Carnot cycle involves two quasistatic isothermal processes where T is kept constant, but κ also changes quasistatically, and two reversible adiabatic processes where T and κ change, but along the adiabatic path, $\kappa = \text{const} * T^2$. The energetic description of this Carnot-like cycle can be summarized as follows.

(i) Isothermal expansion process ($A \rightarrow B$): In this process the stiffness potential trap decreases from $\kappa_4 \rightarrow \kappa_3$ ($\kappa_3 < \kappa_4$) at $T_h = \text{const}$. Besides, $(\Delta E)_{AB} = 0$ and $Q_{AB} = -W_{AB}$,

$$W_{AB} = \frac{k_B T_h}{2} \int_{\kappa_4}^{\kappa_3} \frac{d\kappa}{\kappa} = \frac{k_B T_h}{2} \ln \left(\frac{\kappa_3}{\kappa_4} \right) < 0, \quad (13)$$

$$Q_{AB} = -\frac{k_B T_h}{2} \ln \left(\frac{\kappa_3}{\kappa_4} \right) = \frac{k_B T_h}{2} \ln \left(\frac{\kappa_4}{\kappa_3} \right) > 0. \quad (14)$$

(ii) Adiabatic expansion process ($B \rightarrow C$): An amount of work is performed from $\kappa_3 \rightarrow \kappa_1$ ($\kappa_1 < \kappa_3$), while T changes from $T_h \rightarrow T_c$. As $Q_{BC} = 0$, then $W_{BC} = (\Delta E)_{BC} = k_B(T_h - T_c)$.

(iii) Isothermal compression process ($C \rightarrow D$): This process takes place now for increasing values of κ from $\kappa_1 \rightarrow \kappa_2$ ($\kappa_2 > \kappa_1$), while the system is in contact with a thermal bath at $T = T_c$, where $Q_{CD} = -W_{CD}$; therefore,

$$W_{CD} = \frac{k_B T_c}{2} \int_{\kappa_1}^{\kappa_2} \frac{d\kappa}{\kappa} = \frac{k_B T_c}{2} \ln \left(\frac{\kappa_2}{\kappa_1} \right) > 0, \quad (15)$$

$$Q_{CD} = -\frac{k_B T_c}{2} \ln \left(\frac{\kappa_2}{\kappa_1} \right) < 0. \quad (16)$$

(iv) Adiabatic compression process ($D \rightarrow A$): The last amount of work is extracted from $\kappa_2 \rightarrow \kappa_4$ (with $\kappa_4 > \kappa_2$), in which $Q_{DA} = 0$, and thus $W_{DA} = (\Delta E)_{DA} = k_B(T_h - T_c)$.

The total work performed by this block-thermodynamic cycle becomes $W_{\text{tot}} = W_{AB} + W_{BC} + W_{CD} + W_{DA}$, and according to Eq. (12) the efficiency reads

$$\eta = \frac{W_{\text{tot}}}{Q_{\text{in}}} = \frac{\frac{k_B}{2} [T_h \ln \left(\frac{\kappa_4}{\kappa_3} \right) - T_c \ln \left(\frac{\kappa_2}{\kappa_1} \right)]}{\frac{k_B}{2} T_h \ln \left(\frac{\kappa_4}{\kappa_3} \right)}, \quad (17)$$

where $Q_{\text{in}} = Q_{AB}$. However, from the adiabatic equation and according to Fig. (1), it gives

$$\frac{\kappa_3}{T_h^2} = \frac{\kappa_1}{T_c^2}, \quad \frac{\kappa_4}{T_h^2} = \frac{\kappa_2}{T_c^2}, \quad \text{thus} \quad \frac{\kappa_3}{\kappa_1} = \frac{\kappa_4}{\kappa_2}, \quad (18)$$

and therefore the Carnot-like efficiency becomes

$$\eta_c = \frac{T_h - T_c}{T_h} = 1 - \frac{T_c}{T_h}, \quad (19)$$

which is an expected result. As in the thermodynamic case, the efficiency only depends on the temperatures of the thermal baths.

B. Stirling-like Cycle

In this subsection the analysis of a Stirling-type cycle is presented. The first reported experimental micro-size heat engine was built inspired in this cycle [17]. Analogously to the macroscopic case, this cycle is composed of two isothermal processes linked through two isochoric processes ($\kappa = \text{const}$), as shown in Fig. 2. Each path is swept in a quasistatic way going between two equilibrium states. For a Brownian particle in a harmonic trap, the process is carried out under certain conditions of stiffness and temperature. The energetics in each trajectory can be stated as follows:

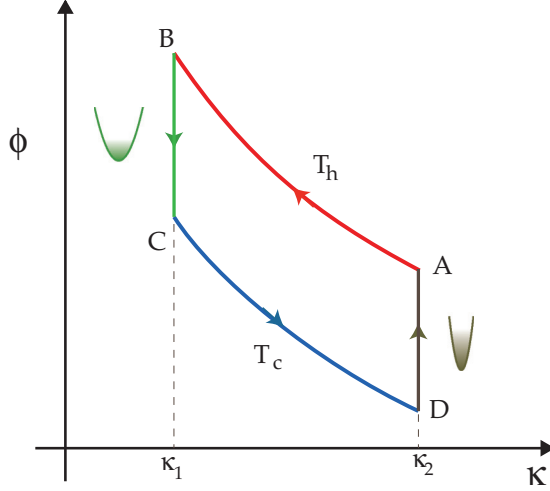


FIG. 2. Φ - κ thermodynamic diagram of a Stirling-like cycle (i) an isothermal expansion ($A \rightarrow B$ path), (ii) an isochoric cooling process ($B \rightarrow C$ path), (iii) an isothermal compression ($C \rightarrow D$ path), and (iv) an isochoric heating process ($D \rightarrow A$ path).

(i) Isothermal expansion process ($A \rightarrow B$): During this process the stiffness of the trap changes from κ_2 to κ_1 ($\kappa_1 < \kappa_2$) and $T_h = \text{const}$. Besides, $\Delta E_{AB} = 0$ and $Q_{AB} = -W_{AB}$, with

$$W_{AB} = \frac{k_B T_h}{2} \ln \left(\frac{\kappa_1}{\kappa_2} \right). \quad (20)$$

(ii) Isochoric process ($B \rightarrow C$): In this case the stiffness remains constant ($\kappa_1 = \text{const}$) and the potential does not change: the work vanishes $W_{BC} = 0$, and the heat is $Q_{BC} = (\Delta E)_{BC}$, such that

$$Q_{BC} = k_B (T_c - T_h) < 0. \quad (21)$$

(iii) Isothermal compression process ($C \rightarrow D$): During this process the stiffness of the trap changes from κ_1 to κ_2 and $T_c = \text{const}$, the colder temperature. In this case, $(\Delta E)_{CD} = 0$ and $Q_{CD} = -W_{CD}$, where

$$W_{CD} = \frac{k_B T_c}{2} \ln \left(\frac{\kappa_2}{\kappa_1} \right). \quad (22)$$

(iv) Isochoric process ($D \rightarrow A$): Similarly to the second branch, the stiffness remains constant ($\kappa_2 = \text{const}$) and the potential does not change: the work vanishes $W_{DA} = 0$ and the heat is $Q_{DA} = (\Delta E)_{DA}$, such that

$$Q_{DA} = k_B (T_h - T_c) > 0. \quad (23)$$

The efficiency of this cycle is given by

$$\begin{aligned} \eta &= \frac{W_{\text{tot}}}{Q_{\text{in}}} = \frac{\frac{k_B}{2} [T_h \ln \left(\frac{\kappa_1}{\kappa_2} \right) - T_c \ln \left(\frac{\kappa_1}{\kappa_2} \right)]}{\frac{k_B}{2} T_h [\ln \left(\frac{\kappa_1}{\kappa_2} \right) + 2(1 - \rho_s)(1 - \frac{T_c}{T_h})]} \\ &= \frac{(1 - \frac{T_c}{T_h}) \ln \left(\frac{\kappa_1}{\kappa_2} \right)}{\ln \left(\frac{\kappa_1}{\kappa_2} \right) + 2(1 - \rho_s)(1 - \frac{T_c}{T_h})} \end{aligned} \quad (24)$$

with $Q_{\text{in}} = Q_{AB} + (1 - \rho_s)k_B(T_h - T_c)$; the parameter ρ_s considers a possible regeneration mechanism, when $\rho_s = 1$ there is a perfect regeneration and $\rho_s = 0$ implies nonregeneration.

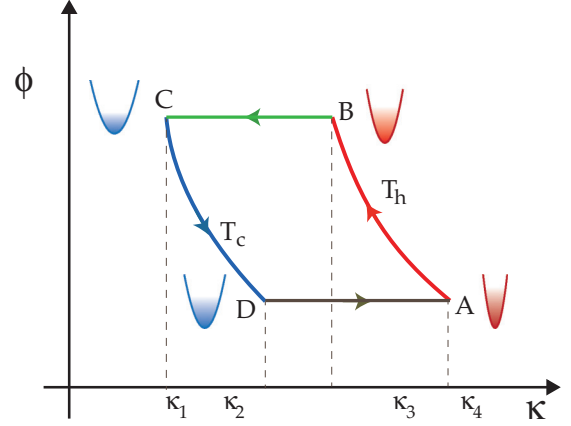


FIG. 3. Φ - κ thermodynamic diagram of an Ericsson-like cycle where (i) an isothermal expansion ($A \rightarrow B$ path), (ii) an isobaric expansion process ($B \rightarrow C$ path), (iii) an isothermal compression ($C \rightarrow D$ path), and (iv) an isobaric compression process ($D \rightarrow A$ path).

As in the macroscopic model, for an ideal regeneration process, the Carnot efficiency is recovered, otherwise, $\eta < \eta_c$.

C. Ericsson-like Cycle

Another cycle that can be constructed using a pair of isotherms is one that includes a pair of isobaric processes, so-called an Ericsson cycle. For the system that concerns us in this work, an Ericsson-like cycle can be implemented as indicated in Fig. 3. There are two quasistatic isothermal processes, where κ changes but T remains constant, and two quasistatic isobaric processes where both κ and T change simultaneously. The four stages of the Ericsson cycle can be stated as follows:

(i) Isothermal expansion process ($A \rightarrow B$): The optical trap is heated at $T_h = \text{const}$, changing from $\kappa_4 \rightarrow \kappa_3$ ($\kappa_3 < \kappa_4$). Besides, $(\Delta E)_{AB} = 0$ and $Q_{AB} = -W_{AB}$, see Eqs. (13) and (14).

(ii) Isobaric expansion process ($B \rightarrow C$): The expanded space for a Brownian particle changes from $\kappa_3 \rightarrow \kappa_1$ ($\kappa_1 < \kappa_3$) and picks up heat at a high constant- Φ_u value from $T_h \rightarrow T_c$. Then, from Eqs. (10) and (11),

$$W_{BC} = \Phi_u \int_{\kappa_3}^{\kappa_1} d\kappa = \Phi_u (\kappa_1 - \kappa_3) = \frac{k_B}{2} (T_c - T_h) < 0, \quad (25)$$

$$Q_{BC} = \frac{k_B}{2} \int_{T_h}^{T_c} dT = \frac{k_B}{2} (T_c - T_h) < 0, \quad (26)$$

where the equationlike state $2\Phi = \langle x^2 \rangle$ has been used to obtain Eq. (26).

(iii) Isothermal compression process ($C \rightarrow D$): The compression space for the colloidal particle is cooled at $T_c = \text{const}$, modifying κ from $\kappa_1 \rightarrow \kappa_2$ ($\kappa_2 > \kappa_1$), as well as $Q_{CD} = -W_{CD}$, see Eqs. (15) and (16).

(iv) Isobaric compression process ($D \rightarrow A$): The compressed space of the optical trap $\kappa_2 \rightarrow \kappa_4$ ($\kappa_4 > \kappa_2$) is carried

out by decreasing the thermal environment at low constant- Φ_I value from $T_c \rightarrow T_h$. Thus,

$$W_{DA} = \Phi_I \int_{\kappa_2}^{\kappa_4} d\kappa = \Phi_I(\kappa_4 - \kappa_2) = \frac{k_B}{2}(T_h - T_c) > 0, \quad (27)$$

$$Q_{DA} = \frac{k_B}{2} \int_{T_c}^{T_h} dT = \frac{k_B}{2}(T_h - T_c) > 0. \quad (28)$$

For this cycle, the total work performed is: $W_{\text{tot}} = W_{AB} + W_{BC} + W_{CD} + W_{DA}$. The total heat input to the cycle is $Q_{\text{in}} = Q_{AB} + \frac{1}{2}k_B(T_h - T_c)$, the one absorbed in the hot isotherm and in the isobaric branch in this case, as in the Stirling cycle, a possible heat regeneration mechanism can be proposed in such a way that $Q_{\text{in}} = Q_{AB} + \frac{1}{2}(1 - \rho_E)k_B(T_h - T_c)$, where ρ_E is associated with the efficiency of the regenerator between isobaric branches. Thus, the expression for the efficiency for this Ericsson-like cycle reads

$$\begin{aligned} \eta &= \frac{W_{\text{tot}}}{Q_{\text{in}}} = \frac{\frac{k_B}{2} [T_h \ln(\frac{\kappa_1}{\kappa_2}) - T_c \ln(\frac{\kappa_4}{\kappa_3})]}{\frac{k_B}{2} T_h [\ln(\frac{\kappa_1}{\kappa_2}) + (1 - \rho_E)(1 - \frac{T_c}{T_h})]} \\ &= \frac{(1 - \frac{T_c}{T_h}) \ln(\frac{\kappa_1}{\kappa_2})}{\ln(\frac{\kappa_1}{\kappa_2}) + (1 - \rho_E)(1 - \frac{T_c}{T_h})}, \end{aligned} \quad (29)$$

since $\kappa_1 = (T_c^2/T_h^2)\kappa_3$ and $\kappa_2 = (T_c^2/T_h^2)\kappa_4$. Additionally, as in the Stirling cycle, $0 \leq \rho_E \leq 1$, where $\rho_E = 1$ would emulate an ideal regeneration, while $\rho_E = 0$ implies null regeneration at the isobaric processes.

IV. LOW-DISSIPATION METHODOLOGY

Once the equilibrium properties of the above three cycles are obtained from Eq. (8), the efficiency at maximum power for each irreversible heat engine will be calculated. The optical trapping techniques use pressure radiation and a focused beam of light to hold in place, or move small-scale objects inside low-density thermal environments [44–47]. In this case, the irreversible average work and irreversible average heat are given respectively by $\langle W \rangle \approx \langle W \rangle_\infty + \frac{\Sigma}{\tau}$ and $\langle Q \rangle \approx \langle Q \rangle_\infty - \frac{T_c \Sigma}{\tau}$, where $\langle W \rangle_\infty$ and $\langle Q \rangle_\infty$ are the average work and average heat, respectively, under equilibrium conditions. Here, the parameter Σ takes into account all information coming from any irreversibility sources, including the time-dependent protocols.

It is important to highlight that within the low-dissipation approach, the adiabatic processes in a macroscopic Carnot heat engine are considered instantaneous, and the irreversible effects are present only in two isothermal processes. In a similar way, the cases of the stochastic Carnot-, Stirling-, and Ericsson-like cycles, consider respectively the isothermic, isochoric, and isobaric processes as instantaneous ones. This means that the relaxation time (time to reach the equilibrium state) of Brownian particles is much faster with respect to the quenching time of the temperature.

A. Performance of an irreversible Carnot-like cycle

In the model of the Carnot cycle, the heat exchanges with the thermal baths only take place in the isothermal branches.

Thus, by following the idea of Esposito *et al.* [30], an ensemble of colloidal particles in contact with thermal baths is now considered. However, each particle is in contact with both reservoirs, the time τ_1 is related to the hot branch, while τ_2 to the cold branch, with τ_1 and τ_2 being finite times. Under this scheme, there is an entropy production per cycle given by

$$\dot{\Sigma} = \frac{\Sigma_1}{\tau_1} + \frac{\Sigma_2}{\tau_2}. \quad (30)$$

The quasistatic regime is reached when $\tau_1 \rightarrow \infty$ as well as $\tau_2 \rightarrow \infty$. That is, there is total exchanged heat due to an amount of dissipated energy for each process. Thus,

$$\begin{aligned} Q_1 &= T_c \left(-\Delta S - \frac{\Sigma_1}{\tau_1} \right), \\ Q_2 &= T_h \left(\Delta S - \frac{\Sigma_2}{\tau_2} \right). \end{aligned} \quad (31)$$

In this weak dissipation approximation, Σ_1 and Σ_2 are associated with the increase of dissipated energy when the isothermal processes are carried out at finite time. Then, from Eqs. (14) and (16), the power output for this Brownian Carnot-like cycle is given by

$$\begin{aligned} P &\equiv \frac{-W}{\tau} = \frac{(T_h - T_c)\Delta S - \left(\frac{T_c \Sigma_1}{\tau_1} + \frac{T_h \Sigma_2}{\tau_2} \right)}{\tau_1 + \tau_2} \\ &= \frac{\frac{k_B}{2}(T_h - T_c) \ln(\frac{\kappa_1}{\kappa_2}) - \left(\frac{T_c \Sigma_1}{\tau_1} + \frac{T_h \Sigma_2}{\tau_2} \right)}{\tau_1 + \tau_2}. \end{aligned} \quad (32)$$

Under these assumptions, a system can achieve the so-called maximum power output regime when the derivatives of P with respect to τ_1 and τ_2 are equal to zero. After substituting Eqs. (14) and (16) into Eq. (32), the physical attainable solution for τ_1 and τ_2 are

$$\begin{aligned} \tau_1^* &= \frac{4T_c \Sigma_1}{(T_h - T_c)k_B \ln(\frac{\kappa_1}{\kappa_2})} \left(1 + \sqrt{\frac{T_h \Sigma_2}{T_c \Sigma_1}} \right), \\ \tau_2^* &= \frac{4T_h \Sigma_2}{(T_h - T_c)k_B \ln(\frac{\kappa_1}{\kappa_2})} \left(1 + \sqrt{\frac{T_c \Sigma_1}{T_h \Sigma_2}} \right). \end{aligned} \quad (33)$$

The same expressions found by Esposito *et al.* [30] for a macroscopic heat engine performing finite-time Carnot cycles. By considering Eqs. (31) and (33), as well as the expression for the efficiency [see Eq. (17)], the efficiency at maximum power regime is obtained as follows:

$$\eta_{\text{MP}} = \frac{(T_h - T_c)(1 + \sqrt{\frac{T_c \Sigma_1}{T_h \Sigma_2}})}{T_h(1 + \sqrt{\frac{T_c \Sigma_1}{T_h \Sigma_2}})^2 + T_c(1 - \frac{\Sigma_1}{\Sigma_2})}. \quad (34)$$

For a symmetric dissipation case ($\Sigma_1 = \Sigma_2$), the well-known Curzon-Ahlborn efficiency is recovered:

$$\eta_{\text{MP}} = 1 - \sqrt{1 - \eta_c} = 1 - \sqrt{\frac{T_c}{T_h}} \equiv \eta_{\text{CA}}. \quad (35)$$

On the other hand, when asymptotic asymmetric cases are considered, $\Sigma_1/\Sigma_2 \rightarrow 0$ lead η_{MP} tends to an upper bound, namely $\eta_{\text{MP}}^u = \eta_{c/2-\eta_c}$. Likewise, if $\Sigma_1/\Sigma_2 \rightarrow \infty$, then η_{MP}

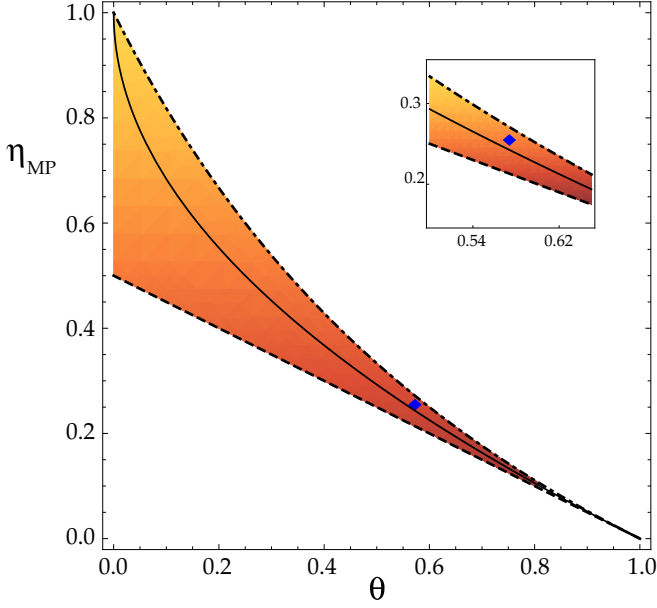


FIG. 4. Efficiency at maximum power of an irreversible Carnot-like cycle as a function of θ . The Curzon-Ahlborn efficiency is denoted by the solid line. Diamond represents the value found in [20]. The upper and lower bound for the asymmetric cases are marked by a dot dashed line and a dashed line, respectively.

tends to a lower bound: $\eta_{\text{MP}}^{\text{I}} = \eta_c/2$. Figure 4 shows η_{MP} as function of θ (where $\theta = T_c/T_h$), and the physically attainable region for the performance of these Brownian systems within the weak dissipation approach in the same way as in [48,49]. The experimental value ($\theta \approx 0.57$, $\eta_{\text{MP}} \approx 0.25$) obtained for the efficiency at maximum power of the Carnot cycle

developed with a Brownian particle [20] is also shown (diamond), and it is located in the physical attainable region (see Fig. 4). This shows that considering a low dissipation model, where all irreversibilities are quantified through the isothermal branches and the adiabatic branches as instantaneous, is consistent with the experimental results.

B. Performance of irreversible Stirling and Ericsson-like cycles

The other two symmetric block-thermodynamic cycles (Stirling and Ericsson) can be also studied within the weak dissipation approximation. From [17], the experiment for a stochastic Stirling heat engine has been performed along two isothermal processes and, due to the difficulties to keep hot and cold reservoirs thermally isolated, the temperature of the surrounding liquid is suddenly changed in the isochoric processes. Therefore, considering the sources of irreversibilities only in the isothermal branches is not an unavailable assumption and the approach of a low dissipation model can be considered for this cycle. Similarly, for the Ericsson cycle it will be assumed that the irreversibilities come from the isothermal branches, while in the isobaric type the thermal bath and the potential stiffness are changed simultaneously and instantaneously. Furthermore, the total ratio of entropy production per cycle of the protocol evolution is expressed by Eq. (30).

Due to the symmetry along isochoric and isobaric processes, the same expression for the entropy transfer as in the Brownian-Carnot cycle is recovered, and therefore, the power output for these Brownian Stirling-like and Ericsson-like cycle models [see Eq. (32)].

For the case of a Brownian Stirling cycle and after substituting Eqs. (31) and (33) into Eq. (24), the efficiency at maximum power output reads:

$$\eta_{\text{MP}}^{\text{S}} = \frac{(T_h - T_c)(1 + \sqrt{\frac{T_h \Sigma_2}{T_c \Sigma_1}})}{T_h(1 + \sqrt{\frac{T_c \Sigma_1}{T_h \Sigma_2}})^2 + T_c(1 - \frac{\Sigma_1}{\Sigma_2}) + 4(1 - R_s)(T_h - T_c)(1 + \sqrt{\frac{T_c \Sigma_1}{T_h \Sigma_2}})}, \quad (36)$$

where $(1 - R_s) = (1 - \rho_s)[\ln(\kappa_1/\kappa_2)]$. For the symmetric dissipation case ($\Sigma_1 = \Sigma_2$), the efficiency at maximum power output of a Stirling-like cycle is

$$\eta_{\text{MP}}^{\text{SS}} = \frac{\eta_{\text{CA}}}{1 + 4(1 - R_s)\eta_{\text{CA}}}. \quad (37)$$

The asymmetric cases for this cycle represent two limits, the first $(\Sigma_1/\Sigma_2) \rightarrow 0$ leads to the upper bound $\eta_{\text{MP}}^{\text{S}} = \eta_c/[2(1+2(1-R_s)\eta_c)-\eta_c]$. Moreover, when $(\Sigma_1/\Sigma_2) \rightarrow \infty$, the lower bound is $\eta_{\text{MP}}^{\text{S}} = \eta_c/2[1+2(1-R_s)\eta_c]$.

Figs. 5(a) and 5(b) depict the behavior of η_{MP} as a function of θ . The energetic performance of these Brownian systems is sketched for two cases. In (a) a low regeneration process ($\rho_s = 0.1$) is emulated while in (b) a high regeneration value ($\rho_s = 0.55$). Now, the experimental value ($\theta \approx 0.82$, $\eta_{\text{MP}}^{\text{S}} \approx 0.075$; represented by diamonds) for a Stirling-like cycle was obtained by [17], and it is in agreement with the physical attainable region for a low regeneration process [Fig. 5(a)].

Likewise, the efficiency at maximum power output regime for an Ericsson-like cycle is obtained from Eqs. (29), (31), and (33):

$$\eta_{\text{MP}}^{\text{E}} = \frac{(T_h - T_c)(1 + \sqrt{\frac{T_c \Sigma_1}{T_h \Sigma_2}})}{T_h(1 + \sqrt{\frac{T_c \Sigma_1}{T_h \Sigma_2}})^2 + T_c(1 - \frac{\Sigma_1}{\Sigma_2}) + 2(1 - R_e)(T_h - T_c)(1 + \sqrt{\frac{T_c \Sigma_1}{T_h \Sigma_2}})}, \quad (38)$$

where $(1 - R_e) = (1 - \rho_e)[\ln(\kappa_1/\kappa_2)]^{-1}$. By assuming the symmetric dissipation ($\Sigma_1 = \Sigma_2$), the efficiency $\eta_{\text{MP}}^{\text{E}}$ is

$$\eta_{\text{MP}}^{\text{ES}} = \frac{\eta_{\text{CA}}}{1 + 2(1 - R_e)\eta_{\text{CA}}}. \quad (39)$$

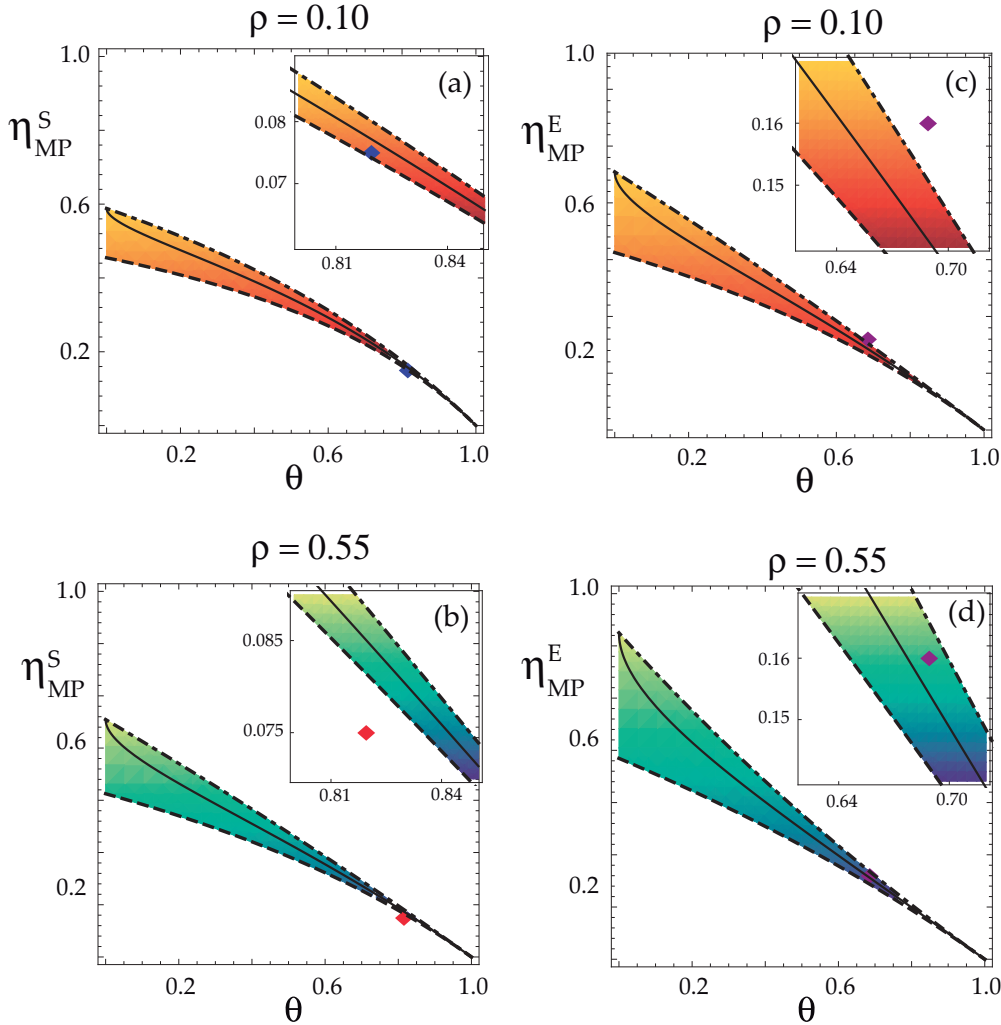


FIG. 5. Efficiency at maximum power of two irreversible cycles [Stirling-like (S) and Ericsson-like (E)] as a function of θ . (a) and (c) with low regeneration ($\rho_s = \rho_e = 0.1$), while (b) and (d) represent high regeneration ($\rho_s = \rho_e = 0.55$). The efficiency for the symmetric dissipation case is denoted by the solid line. Likewise, the upper and lower bound for the asymmetric cases are marked by a dot dashed line and a dashed line, respectively.

Now, the asymmetric cases can also be studied; the first $(\Sigma_1/\Sigma_2) \rightarrow 0$ leads to the upper bound $\eta_{MP}^{+E} = \eta_c/[2(1+(1-R_E)\eta_c)-\eta_c]$. On the other hand, when $(\Sigma_1/\Sigma_2) \rightarrow \infty$, the lower bound is $\eta_{MP}^{-E} = \eta_c/2[1+(1-R_E)\eta_c]$.

In the same way, Figs. 5(c) and 5(d) also depict the behavior of η_{MP} as function of θ . The energetic performance for a proposal of Brownian systems with an Ericsson-like cycle can be sketched for the same two cases: in (c), a low regeneration process ($\rho_e = 0.1$); in (d), a high regeneration ($\rho_e = 0.55$). Note, the general expressions for the performance of Brownian engines at maximum power [see Eqs.(34), (36), and (38)] show an energetic hierarchy, namely $\eta_{MP}^S < \eta_{MP}^E < \eta_{MP}$. The point $(\theta \approx 0.69, \eta_{MP}^E \approx 0.16)$, denoted by diamonds which is shown in Figs. 5(c) and 5(d), has been inferred through a linear interpolation; that is, as $\eta = \eta(\theta)$, it is possible to determine the equation of the line passing through $(\theta_{MP}^S, \eta_{MP}^S)$ and (θ_{MP}, η_{MP}) ; therefore, a qualitative $(\theta_{MP}^E, \eta_{MP}^E)$ can be obtained. Then, by considering the same Brownian system in [17,20], the guidelines to emulate an Ericsson-like cycle

under analogous thermodynamics conditions to the Carnot- and Stirling-like ones can be determined.

Thus, Carnot-, Stirling-, and Ericsson-like cycles exhibit different constrained performance maps (see Fig. 5). These graphs explicitly show that the contribution of the absorbed heat by the isochoric and isobaric paths limit the performance of the Brownian system. Moreover, the existence of a controlled regeneration system would make it possible to compare the maximum power developed by both cycles with the Carnot engine.

V. CONCLUSIONS

In this paper, the strategy of low dissipation for macroscopic heat engines [30] has been used to calculate the efficiency at maximum power of three Brownian heat engines. This is possible with the calculation of the equilibrium thermodynamic properties of the system, around which an approximated expression for the irreversible work and heat has been proposed.

Our proposal shows that in the case of a stochastic Carnot-like heat engine, the efficiency at maximum power is similar to the one reported in [30] for macroscopic heat engines. Also, in the case for which $\Sigma_1 = \Sigma_2$, it recovers the well known Curzon-Alborn efficiency. While in the asymmetric case, an efficiency region is delimited (see Figs. 4 and 5), which in the cases of Stirling- and Ericsson-like cycles depend on the possible so-called regeneration mechanism (Fig. 5). It is important to emphasize that the experimental value of the efficiency, in the Carnot and Stirling cycles, is located in the physical attainable region according to low-dissipation approach, as shown in Fig. 4 and Fig. 5(a), respectively.

From the experimental works [17,20], a possible experimental value for the efficiency in an Ericsson cycle can be

proposed. This allows to establish a hierarchy for the efficiencies of the three cycles given by $\eta_{MP}^S < \eta_{MP}^E < \eta_{MP}$, in a similar way as in the macroscopic heat engines.

Lastly, for a future work, it can be interesting to apply the low-dissipation analysis to other systems, such as chemical systems [50].

ACKNOWLEDGMENTS

O.C.V. thanks the CONACyT-México scholarship. N.S.S. thanks SIP-IPN (México), and G.V.O. acknowledges the support provided by CONACyT-México through the assignment postdoctoral fellowship: Estancias Posdoctorales por México 2022.

-
- [1] P. Reimann, R. Bartussek, R. Häussler, and P. Hänggi, Brownian motors driven by temperature oscillations, *Phys. Lett. A* **215**, 26 (1996).
- [2] P. Reimann, Brownian motors: noisy transport far from equilibrium, *Phys. Rep.* **361**, 57 (2002).
- [3] P. Hänggi, F. Marchesoni, and F. Nori, Brownian motors, *Ann. Phys.* **517**, 51 (2005).
- [4] O. Raz, Y. Subaşı, and C. Jarzynski, Mimicking Nonequilibrium Steady States with Time-Periodic Driving, *Phys. Rev. X* **6**, 021022 (2016).
- [5] D. M. Busiello, C. Jarzynski, and O. Raz, Similarities and differences between non-equilibrium steady states and time-periodic driving in diffusive systems, *New J. Phys.* **20**, 093015 (2018).
- [6] M. O. Magnasco, Forced Thermal Ratchets, *Phys. Rev. Lett.* **71**, 1477 (1993).
- [7] F. Jülicher, A. Ajdari, and J. Prost, Modeling molecular motors, *Rev. Mod. Phys.* **69**, 1269 (1997).
- [8] H. Qian, A simple theory of motor protein kinetics and energetics, *Biophys. Chem.* **67**, 263 (1997).
- [9] M. Bier, Brownian ratchets in physics and biology, *Contemp. Phys.* **38**, 371 (1997).
- [10] A. W. C. Lau, D. Lacoste, and K. Mallick, Nonequilibrium Fluctuations and Mechanochemical Couplings of a Molecular Motor, *Phys. Rev. Lett.* **99**, 158102 (2007).
- [11] R. Perez-Carrasco and J. M. Sancho, Fokker-planck approach to molecular motors, *Eur. PL* **91**, 60001 (2010).
- [12] I. Goychuk, V. Kharchenko, and R. Metzler, Molecular motors pulling cargos in the viscoelastic cytosol: How power strokes beat subdiffusion, *Chem. Phys.* **16**, 16524 (2014).
- [13] Y. Tu and Y. Cao, Design principles and optimal performance for molecular motors under realistic constraints, *Phys. Rev. E* **97**, 022403 (2018).
- [14] W. Hwang and M. Karplus, Structural basis for power stroke vs. brownian ratchet mechanisms of motor proteins, *Proc. Natl. Acad. Sci. USA* **116**, 19777 (2019).
- [15] D. Caballero, S. C. Kundu, and R. L. Reis, The biophysics of cell migration: Biasing cell motion with feynman ratchets, *Biophys. J.* **1**, (2020).
- [16] Y. V. Gulyaev, A. S. Bugaev, V. M. Rozenbaum, and L. I. Trakhtenberg, Nanotransport controlled by means of the ratchet effect, *Phys.-Usp.* **63**, 311 (2020).
- [17] V. Blickle and C. Bechinger, Realization of a micrometre-sized stochastic heat engine, *Nat. Phys.* **8**, 143 (2012).
- [18] J. Gieseler, R. Quidant, C. Dellago, and L. Novotny, Dynamic relaxation of a levitated nanoparticle from a non-equilibrium steady state, *Nat. Nanotechnol.* **9**, 358 (2014).
- [19] I. A. Martínez, É. Roldán, L. Dinis, D. Petrov, and R. A. Rica, Adiabatic Processes Realized with a Trapped Brownian Particle, *Phys. Rev. Lett.* **114**, 120601 (2015).
- [20] I. A. Martínez, É. Roldán, L. Dinis, D. Petrov, J. M. Parrondo, and R. A. Rica, Brownian carnot engine, *Nat. Phys.* **12**, 67 (2016).
- [21] S. de Lorenzo, M. Ribezzi-Crivellari, J. R. Arias-Gonzalez, S. B. Smith, and F. Ritort, A temperature-jump optical trap for single-molecule manipulation, *Biophys. J.* **108**, 2854 (2015).
- [22] A. L. Thorneywork, J. Gladrow, Y. Qing, M. Rico-Pasto, F. Ritort, H. Bayley, A. B. Kolomeisky, and U. F. Keyser, Direct detection of molecular intermediates from first-passage times, *Sci. Adv.* **6**, eaaz4642 (2020).
- [23] K. Sekimoto, *Stochastic Energetics*, Vol. 799 (Springer, Heidelberg, Germany, 2010).
- [24] I. Novikov, The efficiency of atomic power stations (a review), *J. Nucl. Energy* (1954) **7**, 125 (1958).
- [25] F. L. Curzon and B. Ahlborn, Efficiency of a carnot engine at maximum power output, *Am. J. Phys.* **43**, 22 (1975).
- [26] K. H. Hoffmann, J. M. Burzler, and S. Schubert, Endoreversible thermodynamics, *J. Non-Equilib. Thermodyn.* **22**, 311 (1997).
- [27] L. Chen, *Advances in Finite Time Thermodynamics: Analysis and Optimization* (Nova Publishers, New York, USA, 2004).
- [28] B. Andresen, Current trends in finite-time thermodynamics, *Angew. Chem. Int. Ed.* **50**, 2690 (2011).
- [29] A. Bejan, *Entropy Generation Minimization: The Method of Thermodynamic Optimization of Finite-Size Systems and Finite-Time Processes* (CRC Press, New York, USA, 2013).
- [30] M. Esposito, R. Kawai, K. Lindenberg, and C. Van den Broeck, Efficiency at Maximum Power of Low-Dissipation Carnot Engines, *Phys. Rev. Lett.* **105**, 150603 (2010).
- [31] T. Schmiedl and U. Seifert, Optimal Finite-Time Processes In Stochastic Thermodynamics, *Phys. Rev. Lett.* **98**, 108301 (2007).
- [32] Z. C. Tu, Stochastic heat engine with the consideration of inertial effects and shortcuts to adiabaticity, *Phys. Rev. E* **89**, 052148 (2014).

- [33] C. A. Plata, D. Guéry-Odelin, E. Trizac, and A. Prados, Optimal work in a harmonic trap with bounded stiffness, *Phys. Rev. E* **99**, 012140 (2019).
- [34] V. Holubec and A. Ryabov, Efficiency at and near maximum power of low-dissipation heat engines, *Phys. Rev. E* **92**, 052125 (2015).
- [35] C. A. Plata, D. Guéry-Odelin, E. Trizac, and A. Prados, Building an irreversible Carnot-like heat engine with an over-damped harmonic oscillator, *J. Stat. Mech. Theory Exp.* (2020) 093207.
- [36] T. Schmiedl and U. Seifert, Efficiency of molecular motors at maximum power, *Europhys. Lett.* **83**, 30005 (2008).
- [37] S. Rana, P. S. Pal, A. Saha, and A. M. Jayannavar, Single-particle stochastic heat engine, *Phys. Rev. E* **90**, 042146 (2014).
- [38] P. A. Quinto-Su, A microscopic steam engine implemented in an optical tweezer, *Nat. Commun.* **5**, 5889 (2014).
- [39] S. Krishnamurthy, S. Ghosh, D. Chatterji, R. Ganapathy, and A. K. Sood, A micrometre-sized heat engine operating between bacterial reservoirs, *Nat. Phys.* **12**, 1134 (2016).
- [40] K. Sekimoto, F. Takagi, and T. Hondou, Carnots cycle for small systems: Irreversibility and cost of operations, *Phys. Rev. E* **62**, 7759 (2000).
- [41] T. R. Gingrich, G. M. Rotskoff, G. E. Crooks, and P. L. Geissler, Near-optimal protocols in complex nonequilibrium transformations, *Proc. Natl. Acad. Sci. USA* **113**, 10263 (2016).
- [42] I. A. Martínez, É. Roldán, J. M. R. Parrondo, and D. Petrov, Effective heating to several thousand kelvins of an optically trapped sphere in a liquid, *Phys. Rev. E* **87**, 032159 (2013).
- [43] L. Dinis, I. A. Martínez, É. Roldán, J. M. R. Parrondo, and R. A. Rica, Thermodynamics at the microscale: From effective heating to the Brownian Carnot engine, *J. Stat. Mech. Theory Exp.* (2016) 054003.
- [44] A. Ashkin, J. M. Dziedzic, and T. Yamane, Optical trapping and manipulation of single cells using infrared laser beams, *Nature (London)* **330**, 769 (1987).
- [45] A. Ashkin and J. M. Dziedzic, Optical trapping and manipulation of viruses and bacteria, *Science* **235**, 1517 (1987).
- [46] K. Svoboda, C. F. Schmidt, D. Branton, and S. M. Block, Conformation and elasticity of the isolated red blood cell membrane skeleton, *Biophys. J.* **63**, 784 (1992).
- [47] M. C. Leake, D. Wilson, M. Gautel, and R. M. Simmons, The elasticity of single titin molecules using a two-bead optical tweezers assay, *Biophys. J.* **87**, 1112 (2004).
- [48] L. Chen and Z. Yan, The effect of heat-transfer law on performance of a two-heat-source endoreversible cycle, *J. Chem. Phys.* **90**, 3740 (1989).
- [49] B. Gaveau, M. Moreau, and L. S. Schulman, Stochastic Thermodynamics and Sustainable Efficiency in Work Production, *Phys. Rev. Lett.* **105**, 060601 (2010).
- [50] D. M. Busiello, S. Liang, F. Piazza, and P. De Los Rios, Dissipation-driven selection of states in non-equilibrium chemical networks, *Commun. Chem.* **4**, 16 (2021).